

Ultrasonic attenuation in an orthorhombic anisotropic superconductor

W. C. Wu

Department of Physics, National Taiwan Normal University, Taipei 11650, Taiwan

J. P. Carbotte

Department of Physics and Astronomy, McMaster University, Hamilton, Ontario, Canada L8S 4M1

(Received 19 May 1999)

We show that ultrasound attenuation in a clean two-dimensional orthorhombic superconductor can be used to get information separately, on band-structure anisotropy, and on the relative magnitude of a subdominant s -wave component to the dominant d -wave gap. An angular sweep as a function of orientation of the in-plane attenuated sound momentum will exhibit a twofold pattern. Using a simplified one-band model of the electronic structure with anisotropic effective masses in the plane, we illustrate that the maximum in the attenuation occurs when the direction of the sound is perpendicular to the direction of the Fermi velocity at the nodes. This is not the same as the direction of the nodes in the gap except for the case of a circular Fermi surface. Nevertheless, with the same analysis, nodal directions can be determined as well as band and gap anisotropy parameters and the ratio of gap magnitude to Fermi energy. [S0163-1829(99)01545-3]

I. INTRODUCTION

The topic of anisotropic or unconventional superconductivity is currently of great interest with regard to the high- T_c copper oxide in which the superconductivity is believed to reside in the two-dimensional CuO_2 planes and the energy gap is known to exhibit $d_{x^2-y^2}$ symmetry. A complication arises in $\text{YBa}_2\text{Cu}_3\text{O}_7$ (YBCO) because it is orthorhombic rather than tetragonal with CuO chains along one of the planar axes. These chains are conducting and participate in the superconductivity. In this case, the gap can possess in addition to a dominant $d_{x^2-y^2}$ piece a subdominant s -wave component,¹⁻⁴ which shifts the node off the main diagonals. Additional effects of band anisotropy, i.e., orthorhombicity, include important changes in residual density of states in the presence of elastic impurity scattering.^{5,6} A finite density of states at zero energy can drastically affect the observed low-temperature properties that depend mainly on the behavior around the gap nodes. To understand these effects better, it is important to have more experiments that reveal details of gap and band anisotropies.

In this paper, we show that ultrasonic attenuation^{7,8} can be used to determine the anisotropy exhibited in high- T_c cuprates. An angular sweep of the sound momentum will exhibit a twofold symmetry and through analysis of the observed pattern, one can (i) measure the angular position of the gap nodes, (ii) measure the ratio of the maximum gap to the Fermi energy, and (iii) extract the anisotropy due to the band structure and the gap symmetry *separately*.

The previous related work of Vekhter *et al.*⁹ deals only with the tetragonal case and so the issues of band and gap anisotropies, which are central in this paper, do not arise. The work of Kostur *et al.*⁷ and of Wolenski and Swihart⁸ both assume the limit of zero gap to Fermi energy ratio and so predict an exponential temperature dependence at sufficiently low T in contrast to our finding that it is linear in accordance with the work of Coppersmith and Klemm¹⁰ and of Ref. 9. The recent work of Moreno and Coleman¹¹ treats the dirty limit (diffusive case), while here we deal with the

clean limit (ballistic case). Experimental issues related to the detection of effects described in the previous work and elaborated upon and extended here, have been raised by Leibowitz.¹² Ultrasonic attenuation measurements give an alternative bulk measurement method for determining gap anisotropy, which does not depend on nonlinear effects as does the nonlinear Meissner effect, which has yet to yield results of Ref. 13.

The format of this paper is as follows. In Sec. II, we derive the formalism and introduce our model to study the ultrasonic attenuation for an orthorhombic anisotropic superconductor. In Sec. III, we present our major results and show explicitly that ultrasonic attenuation is useful in determining the gap symmetry and band-structure anisotropies exhibited in high- T_c cuprates. In Sec. IV, we discuss the result in the case when the ratio $\Delta(0)/\epsilon_F$ is negligibly small [here $\Delta(0)$ is the maximum gap magnitude at $T=0$ and ϵ_F is the Fermi energy] and in Sec. V, we give a brief summary. Throughout this paper, we have taken $\hbar = k_B = 1$ for brevity.

II. FORMALISM AND MODEL

To study sound propagation in high- T_c superconductors, one needs first to clarify whether a collisionless or hydrodynamic regime is appropriate. Though the coherence length of Cooper pairs is short in high- T_c cuprates, the scattering of phonons with electrons can be in the collisionless regime ($ql \gg 1$ with q the momentum wave vector of phonons and l the mean free path of electrons, which can be of order a few microns in recent samples¹⁴), i.e., in the *clean* limit. As a result, the damping rate for phonon propagation $\alpha_\lambda \equiv \text{Im} \omega_\lambda(\mathbf{q})$ (λ denotes the polarization) is directly proportional to the imaginary part of the phonon-coupled density-density response function $\chi(\mathbf{q}, \omega)$ for electrons.

For a superconductor, it is straightforward to calculate the response function to lowest order $\chi \equiv GG - FF$, which involves both the normal (G) and anomalous (F) single-particle Green's functions. For sound attenuation, we are in-

terested in small phonon momentum \mathbf{q} and frequency ω , which are governed by the sound velocity c_λ via $\omega_\lambda = c_\lambda q_\lambda$. In this regime, the imaginary part of χ is given by (see, for example, Refs. 15–17)

$$\text{Im } \chi(\mathbf{q}, \omega) = \omega \sum_{\mathbf{k}} |g(\mathbf{k})|^2 \frac{\varepsilon_{\mathbf{k}}^2}{E_{\mathbf{k}}^2} \left[-\frac{\partial f(E_{\mathbf{k}})}{\partial E_{\mathbf{k}}} \right] \delta(E_{\mathbf{k}+\mathbf{q}} - E_{\mathbf{k}}), \quad (1)$$

where $E_{\mathbf{k}} = [\varepsilon_{\mathbf{k}}^2 + \Delta_{\mathbf{k}}^2]^{1/2}$ is the quasiparticle excitation spectrum with $\varepsilon_{\mathbf{k}}$ the particle band energy and $\Delta_{\mathbf{k}}$ the superconducting gap. The function $g(\mathbf{k})$ is the electron-phonon coupling. Terms involving creation or destruction of two quasiparticles are obviously absent in Eq. (1). In conventional s -wave superconductors, this is obviously due to the fact that the phonon energy is small compared to the minimum energy 2Δ required to break up a Cooper pair. For an anisotropic superconductor considered here, the condition holds except for small regions around the nodes, which gives only minor correction relative to the rest.

When \mathbf{q} is small, the δ function in Eq. (1) can be approximated by

$$\delta(E_{\mathbf{k}+\mathbf{q}} - E_{\mathbf{k}}) \approx \delta\left(\frac{\partial E_{\mathbf{k}}}{\partial \mathbf{k}} \cdot \mathbf{q}\right) = \delta\left(\frac{\varepsilon_{\mathbf{k}}}{E_{\mathbf{k}}} \mathbf{v} \cdot \mathbf{q} + \frac{\Delta_{\mathbf{k}}}{E_{\mathbf{k}}} \frac{\partial \Delta_{\mathbf{k}}}{\partial \mathbf{k}} \cdot \mathbf{q}\right), \quad (2)$$

where the electron velocity $\mathbf{v} \equiv \partial \varepsilon_{\mathbf{k}} / \partial \mathbf{k}$ is calculated dominantly on the Fermi surface due to the Fermi function factor in Eq. (1). One can estimate the order of the ratio of the second to the first term in Eq. (2). It is $\sim \Delta(0)/\varepsilon_F$ (see later). For an isotropic s -wave superconductor, however, the second term vanishes and thus only the portion of the Fermi surface perpendicular to \mathbf{q} will contribute to the integration in Eq. (1). For unconventional superconductors such as high- T_c cuprates, the second term does contribute and how important it is depends on the ratio of $\Delta(0)/\varepsilon_F$, which for $\text{YB}_2\text{C}_3\text{O}_7$ is roughly 0.05–0.2. Therefore, the second term is important.

Layered YBCO has two CuO_2 planes and one CuO chain within a unit cell. One is therefore involved in a three-layer problem. To capture the essential physics however in the simplest possible way, we model YBCO by a single band with an elliptical Fermi surface,^{5,6}

$$\varepsilon_{\mathbf{k}} = \frac{k_x^2}{2m_x} + \frac{k_y^2}{2m_y} - \varepsilon_F, \quad (3)$$

where the effective mass $m_x > m_y$ because the CuO chain is taken to be along the k_y axis. This models naturally a case for which the electronic transport is easier along the y axis than along the x axis. A superconducting gap of the form

$$\Delta_{\mathbf{k}}(T) = \Delta(T) (\hat{k}_x^2 - \hat{k}_y^2 + s) \quad (4)$$

is assumed, which has a dominant $d_{x^2-y^2}$ -wave component and a small s -wave admixture. In Eq. (4), \hat{k}_μ ($\mu = x, y$) are the μ component of the unit vector $\hat{\mathbf{k}}$ defined on the Fermi surface. We note that the s component, though small, can in general be positive or negative.

To evaluate Eqs. (1) and (2) for an elliptical band (3), it is convenient to apply the transformation

$$k_\mu \equiv k'_\mu \sqrt{\frac{2m_\mu}{m_x + m_y}} \quad (\mu = x, y), \quad (5)$$

so that the band energies (3) are transformed from $\varepsilon_{\mathbf{k}} \rightarrow \varepsilon_{\mathbf{k}'}$ $\equiv (k_x'^2 + k_y'^2)/(m_x + m_y) - \varepsilon_F$, which has a cylindrical Fermi surface. In this frame, one can define a Fermi wave number k_F , which satisfies $k_F^2/(m_x + m_y) = \varepsilon_F$ and a Fermi speed given by $v_F = (2k_F)/(m_x + m_y)$. Moreover, of most importance, the momentum \mathbf{k} sum in Eq. (1) can be replaced by an integration $\sum_{\mathbf{k}} \rightarrow \sum_{\mathbf{k}'} \equiv N(0) \int_{-\infty}^{\infty} d\varepsilon \int_0^{2\pi} d\phi / 2\pi$, where $N(0) \equiv (m_x + m_y)/2\pi$ is the density of states and ϕ is the azimuthal angle in the \mathbf{k}' frame. In a similar manner, the gap function (4) is transformed to

$$\Delta_{\mathbf{k}} \rightarrow \Delta_{\mathbf{k}'} = \Delta(\phi) = \Delta(T) f(\phi) \quad (6)$$

on the transformed Fermi surface, where

$$f(\phi) = \frac{\cos(2\phi) + \alpha}{1 + \alpha \cos(2\phi)} + s, \quad (7)$$

in which α is positive and defined by

$$\alpha \equiv \frac{m_x - m_y}{m_x + m_y}. \quad (8)$$

A cylindrical Fermi surface corresponds to $m_x = m_y$ or $\alpha = 0$. The two parameters α and s correspond to band-structure anisotropy and gap-symmetry anisotropy, respectively, in our simplified model, and can be fit to experiments. The critical angle ϕ^c , which makes $f(\phi)$ in Eq. (7) vanish, is

$$\phi^c = \tan^{-1} \left[\sqrt{\frac{(1+\alpha)(1+s)}{(1-\alpha)(1-s)}} \right] \quad (9)$$

in the region of $(0, \pi/2)$. It is worth noting that when $\alpha = -s$, $\phi^c = \pi/4$. This corresponds to the interesting case for which the effect due to band-structure anisotropy is compensated for by the gap-symmetry anisotropy (see Ref. 6). While in Eq. (9), the compensation is exact, other properties still differ from the $\alpha = s = 0$ case.⁵

III. ULTRASOUND ATTENUATION

Using the above \mathbf{k}' transformation and after carrying out the energy integration, the ratio of longitudinal ultrasonic attenuation in the superconducting state to its normal state value ($\Delta_{\mathbf{k}} = 0$) is reduced to⁹

$$\frac{\alpha_s}{\alpha_n} = \frac{\left\langle \frac{\varepsilon^2(\phi)}{4TE(\phi)|\mathbf{v} \cdot \mathbf{q}|} \cosh^{-2} \left[\frac{E(\phi)}{2T} \right] \right\rangle}{\langle \delta(\mathbf{v} \cdot \mathbf{q}) \rangle}, \quad (10)$$

where $\langle A \rangle \equiv \int_0^{2\pi} d\phi A / 2\pi$ denotes a Fermi-surface average. In the denominator of Eq. (10) responsible for the normal state, only two points on the Fermi surface satisfy $\mathbf{v} \cdot \mathbf{q} = 0$ for each \mathbf{q} and contribute to the average (see Fig. 1). But this is not the case for the superconducting state in the numerator of Eq. (10). In Eq. (10), $E(\phi) = [\varepsilon^2(\phi) + \Delta^2(\phi)]^{1/2}$, where $\Delta(\phi)$ is given in Eq. (6) and

$$\varepsilon(\phi) = -\Delta(\phi) \frac{\mathbf{u} \cdot \mathbf{q}}{\mathbf{v} \cdot \mathbf{q}}, \quad (11)$$

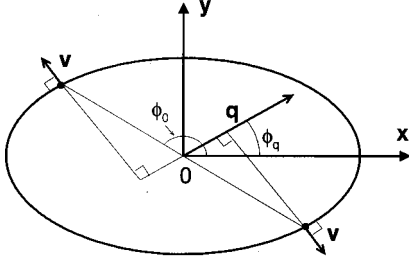


FIG. 1. Schematic diagram of Fermi velocities \mathbf{v} and momentum transfer \mathbf{q} of ultrasound in the case of an elliptical Fermi surface.

in which $\mathbf{u} \equiv \partial \Delta_{\mathbf{k}} / \partial \mathbf{k}$ and $\mathbf{v} \equiv \partial \varepsilon_{\mathbf{k}} / \partial \mathbf{k}$, both viewed in the transformed \mathbf{k}' frame. We note that the effect of anisotropy in the electron-phonon coupling g has been ignored in Eq. (10), which may lead to minor corrections, but is beyond the scope of this paper. In the following, we will use the notation that ϕ_q denotes the angle of the sound propagation momentum \mathbf{q} .

When $T \ll T_c$, we find approximately (see Ref. 9)

$$\frac{\alpha_s}{\alpha_n} \approx 2 \ln 2 \frac{T}{\epsilon_F} \gamma \frac{|\partial h_1(\phi, \phi_q) / \partial \phi|_{\phi=\phi_0}}{|df(\phi) / d\phi|_{\phi=\phi^c}} \times \left\{ \frac{h_2^2(\phi^c, \phi_q)}{[h_1^2(\phi^c, \phi_q) + \gamma^2 h_2^2(\phi^c, \phi_q)]^{3/2}} + (\phi^c \rightarrow -\phi^c) \right\}, \quad (12)$$

where $\gamma \equiv \Delta(0) / \epsilon_F$,

$$h_1(\phi, \phi_q) \equiv \frac{\mathbf{v} \cdot \mathbf{q}}{q v_F} = \frac{\cos \phi \cos \phi_q}{\sqrt{1+\alpha}} + \frac{\sin \phi \sin \phi_q}{\sqrt{1-\alpha}}, \quad (13)$$

and

$$h_2(\phi, \phi_q) \equiv \frac{\mathbf{u} \cdot \mathbf{q}}{2q \Delta(0) / k_F} = \left[\frac{\sin 2\phi(1-\alpha^2)}{(1+\alpha \cos 2\phi)^2} \right] \times \left(\frac{\sin \phi \cos \phi_q}{\sqrt{1+\alpha}} - \frac{\cos \phi \sin \phi_q}{\sqrt{1-\alpha}} \right). \quad (14)$$

As shown clearly in Eq. (12) and as is the case for many properties of an unconventional superconductor, the low-temperature ultrasonic attenuation is mainly determined by their behavior around the nodes ($\phi \approx \phi^c$). Moreover in Eq. (12), ϕ_0 is the angle of the electronic velocity \mathbf{v} perpendicular to \mathbf{q} . One can easily find that

$$\phi_0 = \cot^{-1} \left[-\sqrt{\frac{1+\alpha}{1-\alpha}} \tan \phi_q \right] \quad (15)$$

in the range $(\pi/2, \pi)$. In Fig. 1, we sketch the diagram of Fermi velocities \mathbf{v} and momentum transfer \mathbf{q} of ultrasonic attenuation in the case of an elliptical Fermi surface. The highlight is that while \mathbf{v} is perpendicular to \mathbf{q} , the angle $(\phi_0 - \phi_q)$ between the momentum defining \mathbf{v} and the vector \mathbf{q} is not in general $\pi/2$, except for a circular Fermi surface.

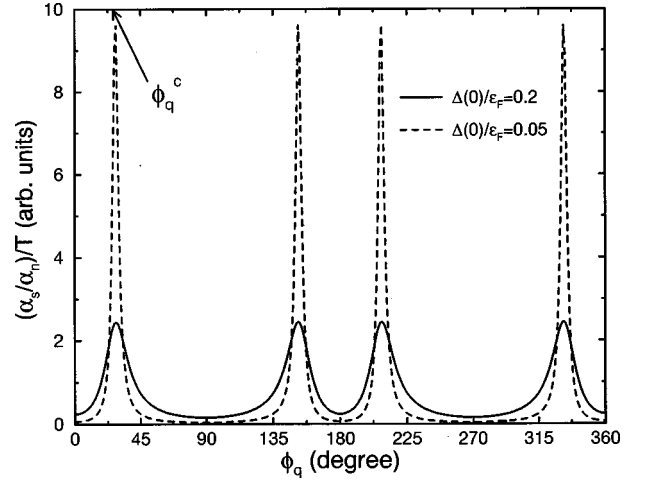


FIG. 2. Low-temperature slopes of α_s / α_n with respect to temperature [see Eq. (12)] vs the angle of momentum transfer for a $d + s$ -wave superconductor with an elliptical Fermi surface. Two different $\Delta(0) / \epsilon_F$ ratios are chosen and we have set $\alpha = 0.4$ and $s = -0.2$.

Figure 2 shows the low-temperature value of $(\alpha_s / \alpha_n) / T$ [using Eq. (12)] as a function of the angle of sound momentum transfer. We choose two different values of $\Delta(0) / \epsilon_F$ and fix $\alpha = 0.4$ and $s = -0.2$. These values of α and s were chosen previously⁶ to fit the observed zero-temperature value of the penetration depth in the a and b direction and observed low-temperature slopes.¹⁸⁻²⁰ The peaks deviate from $\phi_q = \pi/4$ due to the presence of α and s anisotropies. In the vicinity of slope maxima, the larger the ratio $\Delta(0) / \epsilon_F$, the smaller the slope magnitude. In contrast, near the antinodes ($\phi_q \approx 0$ or $\pi/2$), the larger the value of $\Delta(0) / \epsilon_F$, the larger the slope magnitude.⁹ In the following, we focus on how we might extract values for α and s components separately from ultrasonic attenuation measurements.

A. Maximum ratio slopes

The measured critical angle ϕ_q^c (see Fig. 2) where the slope of attenuation ratio $(\alpha_s / \alpha_n) / T$ is maximum corresponds to $h_1(\pm \phi^c, \phi_q^c) = 0$ in Eq. (12). Substituting ϕ^c in Eq. (9) into Eq. (13), we find

$$\phi_q^c = \tan^{-1} \left[\frac{1-\alpha}{1+\alpha} \sqrt{\frac{1-s}{1+s}} \right] \quad (16)$$

in the range of $(0, \pi/2)$. Therefore finding of angles at which the slope of the ultrasonic attenuation ratio is maximum can lead to information on the gap and the band-structure anisotropy. At this stage, α and s cannot be extracted separately, but we will show in the next section that this can be done.

On the other hand, the magnitude of the maximum ratio slope at ϕ_q^c at low temperatures is calculated to be

$$\left. \frac{(\alpha_s / \alpha_n)}{T} \right|_{\phi_q = \phi_q^c} = \frac{\ln 2}{\Delta(0)} \left[\frac{\epsilon_F}{\Delta(0)} \right] \frac{1-\alpha^2}{(1-s^2)(1+\alpha s)^2}. \quad (17)$$

As indicated in Eq. (17), in principle one can obtain the ratio of $\Delta(0) / \epsilon_F$ from the magnitude of maximum slopes when $\Delta(0)$, α , and s are known. In Fig. 3 we study the effect of

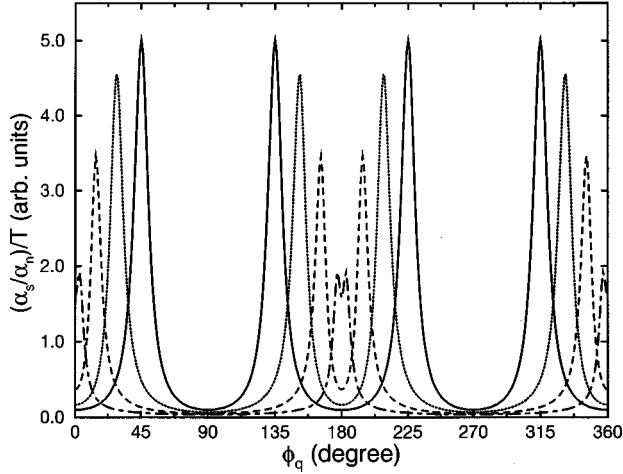


FIG. 3. The dependence of α (band structure orthorhombicity) on the low-temperature slopes, $(\alpha_s/\alpha_n)/T$. We have taken $\Delta(0)/\epsilon_F=0.1$ and $s=0$. Solid, dotted, dashed, and dot-dashed lines are for $\alpha=0, 0.3, 0.6$, and 0.9 , respectively.

band-structure orthorhombicity (we set $s=0$ and vary α) on the ratio slopes $(\alpha_s/\alpha_n)/T$. One finds that the value of α affects not only the angular positions of ratio maxima, but also the magnitude. The fourfold symmetry in case of $\alpha=0$ is broken and reduced to a twofold symmetry when $\alpha \neq 0$. In the case of extremely large α value, the two maximum slope peaks can combine into a single peak at $\phi_q = \pi$.

B. Antinode

As seen in Figs. 2 or 3, the curve is asymmetric on the two sides of the critical angle, ϕ_q^c . The low-temperature ratio of the attenuation ratios at the two antinodes ($\phi_q=0, \pi/2$) is found to be

$$\frac{\alpha_s/\alpha_n(\phi_q=0)}{\alpha_s/\alpha_n(\phi_q=\pi/2)} = \left[\frac{(1+\alpha)(1+s)}{(1-\alpha)(1-s)} \right]^{5/2}. \quad (18)$$

Equation (18) provides another way to test both the gap symmetry and band-structure anisotropy. The two measurements of ϕ_q^c [using Eq. (16)] and the ratio at antinodes [using Eq. (18)] allow one to extract the values of α and s separately. When α and s are known, the ratio of $\Delta(0)/\epsilon_F$ can be extracted from Eq. (17).

To end this section, it is noted that the angle ϕ_{node} , which corresponds to the real gap nodes in the original \mathbf{k} frame, is given by

$$\phi_{\text{node}} = \tan^{-1} \left[\sqrt{\frac{1+s}{1-s}} \right] \quad (19)$$

in the region of $(0, \pi/2)$. Clearly ϕ_{node} is independent of α as expected. Extraction of the s component of the gap using the method mentioned above will allow identification of the angular position of gap nodes in the original frame.

IV. CASE OF $\Delta(0)/\epsilon_F \rightarrow 0$

In this section, we consider the limit when $\Delta(0)/\epsilon_F$ is negligibly small. In this case, the second term in the δ function of Eq. (2) is dropped and, consequently, the ratio of

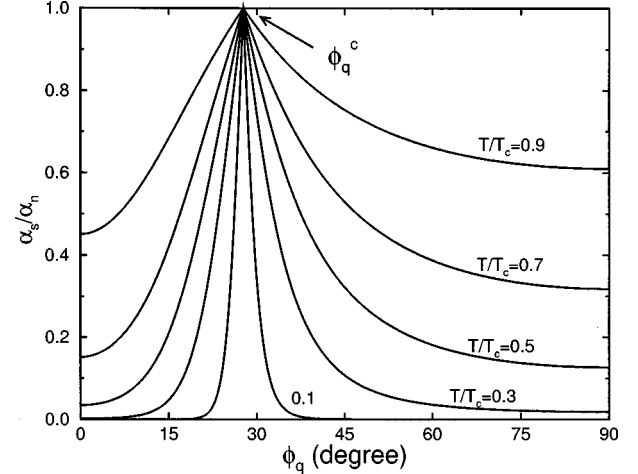


FIG. 4. The ratio of ultrasonic attenuation in superconducting to normal state as a function of the angle of momentum transfer [using Eq. (21)]. Here $\alpha=0.4$ and $s=-0.2$.

attenuation coefficients is reduced to¹⁵

$$\frac{\alpha_s}{\alpha_n} = \frac{\langle 2 \delta(\mathbf{v} \cdot \mathbf{q}) f(|\Delta_{\mathbf{k}'}|) \rangle}{\langle \delta(\mathbf{v} \cdot \mathbf{q}) \rangle}. \quad (20)$$

Clearly in Eq. (20), for both α_s and α_n , only two points on the Fermi surface satisfy $\mathbf{v} \cdot \mathbf{q} = 0$ and contribute for a two-dimensional superconductor (see Fig. 1). Thus, one simply obtains

$$\frac{\alpha_s}{\alpha_n} = 2f(|\Delta(\phi_q)|) = \frac{2}{e^{|\Delta(\phi_0)|/T} + 1}, \quad (21)$$

where ϕ_0 is a function of ϕ_q and is governed by Eq. (15). The key difference between Eq. (21) and Eq. (12) is that the latter was linear in T , while the former is exponential in T . One cannot obtain Eq. (21) by simply taking the asymptotic limit in Eq. (12). This is because the former is an exact result, while the latter is approximate.

The form of Eq. (21) is familiar for a conventional s -wave superconductor. The difference in the present case is that the gap $\Delta(\phi_q)$ exhibits an angular dependence, which in turn is reflected in the angular dependence of the attenuation. In Fig. 4, we plot Eq. (21) vs ϕ_q at different temperatures with fixed $\alpha=0.4$ and $s=-0.2$ (same values as used in Fig. 2). The temperature dependence of $\Delta(T)$ was assumed to be given by the BCS value with $2\Delta(0)/T_c=3.52$. In fact, in the present small $\Delta(0)/\epsilon_F$ limit, the temperature dependence of $\Delta(T)$ can be measured directly by ultrasound attenuation experiment (see later).

Comparing Fig. 2 with Fig. 4, the peaks appear at the same critical angle ϕ_q^c [see Eq. (16)]. Thus, the second term of Eq. (2) has no effect on the peak positions of ultrasound attenuation. In Eq. (21), the maximum attenuation ratio α_s/α_n (unity) corresponds to $\Delta(\phi_0)=0$ (gap nodes) to which $\phi_0 = \pi - \phi^c$ [by using Eqs. (9), (15), and (16)]. Second, we found that the absolute value of the angular slope at the critical angle (same for two sides) is given by

$$\left. \frac{\partial(\alpha_s/\alpha_n)}{\partial\phi_q} \right|_{\phi_q=\phi_q^c} = \frac{\Delta(T)}{T} \frac{\sqrt{1-s^2}(1+\alpha^2+2\alpha s)}{1-\alpha^2}. \quad (22)$$

Therefore, in the case when the ratio $\Delta(0)/\epsilon_F$ is small, the angular slope of α_s/α_n at the critical value can be used to measure the temperature dependence of the superconducting gap provided that α and s are known. Finally, while the slopes vanish at the two antinodes $\phi_q=0$ and $\pi/2$, the ratio of the values at these angles are

$$\frac{\alpha_s/\alpha_n(\phi_q=0)}{\alpha_s/\alpha_n(\phi_q=\pi/2)} = \frac{1 + \exp\left[\frac{\Delta(T)}{T}(1+s)\right]}{1 + \exp\left[\frac{\Delta(T)}{T}(1-s)\right]}, \quad (23)$$

which is independent of α , the band-structure anisotropy parameter.

In summary in the case when $\Delta(0)/\epsilon_F$ is small, a measurement of the attenuation ratios at the two antinodes will give direct information on the s -wave admixture, assuming that the temperature dependence of the gap magnitude is found from the measurements of slopes at the critical angle. With a knowledge of the s -component in the gap, the nodal angle of the gap can be determined via Eq. (19) and the value of α can be determined from the measurement of ϕ_q^c using Eq. (16).

V. CONCLUSION

In this paper, we have studied the low-temperature ($T \ll T_c$) ultrasound attenuation in a clean $d+s$ -wave supercon-

ductor with an orthorhombic band structure. The critical angle defining the direction of the momentum of the propagating sound wave at which the attenuation ratio of superconducting to normal state ratio α_s/α_n is maximum depends strongly on the gap symmetry anisotropy and band-structure anisotropy. Moreover, the magnitude of these critical attenuation ratios are also strongly dependent on these anisotropies. We have shown that by making an angular sweep of the attenuated sound wave momentum, the angular position of gap node, the ratio of the maximum gap to the Fermi energy, and separately the band-structure and gap-symmetry anisotropy parameters can be extracted. Contrary to the expectation for a tetragonal d -wave superconductor, such an angular sweep possesses only a twofold instead of a fourfold symmetry and the angle at which the maximum in attenuation occurs is not equal to the nodal directions. Instead it is when the direction of the sound wave is perpendicular to the direction of the electron Fermi velocity at the nodes.

ACKNOWLEDGMENTS

We thank E. Schachinger, I. Vekhter, E. Nicol, J. X. Li, and T. K. Lee for stimulating discussions. W.C.W. is grateful for the support of National Science Council (NSC) of Taiwan under Grant No. 88-2112-M-003-004 and the hospitality of Institute of Physics, Academia Sinica. J.P.C. acknowledges the support from Natural Sciences and Engineering Research Council (NSERC) of Canada and Canadian Institute for Advanced Research (CIAR).

-
- ¹A.G. Sun, D.A. Gajewski, M.B. Maple, and R.C. Dynes, Phys. Rev. Lett. **72**, 2267 (1994); Phys. Rev. B **54**, 6734 (1996).
²K.A. Kouznetsov, A.G. Sun, B. Chen, A.S. Katz, S.R. Bahcall, J. Clarke, R.C. Dynes, D.A. Gajewski, S.H. Han, M.B. Maple, J. Giapintzakis, J.-T. Kim, and D.M. Ginsberg, Phys. Rev. Lett. **79**, 3050 (1997).
³H. Aubin, K. Behnia, M. Ribault, R. Gagnon, and L. Taillefer, Phys. Rev. Lett. **78**, 2624 (1997).
⁴R. Kleiner, A.S. Katz, A.G. Sun, R. Summer, D.A. Gajewski, S.H. Han, S.I. Woods, E. Dantsker, B. Chen, K. Char, M.B. Maple, R.C. Dynes, and J. Clarke, Phys. Rev. Lett. **76**, 2161 (1996).
⁵H. Kim and E.J. Nicol, Phys. Rev. B **52**, 13 576 (1995).
⁶W.C. Wu, D. Branch, and J.P. Carbotte, Phys. Rev. B **58**, 3417 (1998).
⁷V.N. Kostur, J.K. Bhattacharjee, and R.A. Ferrell, Pis'ma Zh. Éksp. Teor. Fiz. **61**, 552 (1995) [JETP Lett. **61**, 560 (1995)].
⁸T. Wolenski and J.C. Swihart, Physica C **253**, 266 (1995).
⁹I. Vekhter, E. Nicol, and J.P. Carbotte, Phys. Rev. B **59**, 7123 (1999).
¹⁰S. Coppersmith and R.A. Klemm, Phys. Rev. Lett. **56**, 1870 (1986).
¹¹J. Moreno and P. Coleman, Phys. Rev. B **53**, R2995 (1996).
¹²J.R. Leibold, Physica C **259**, 304 (1996).
¹³M.-R. Li, P.J. Hirschfeld, and P. Wölfle, Phys. Rev. Lett. **81**, 5640 (1998).
¹⁴A. Hosseini, R. Harris, S. Kamal, P. Dosanjh, J. Preston, R. Liang, W.N. Hardy, and D.A. Bonn, cond-mat/9811041 (unpublished).
¹⁵V.L. Pokrovskii, Zh. Éksp. Teor. Fiz. **40**, 898 (1961) [Sov. Phys. JETP **13**, 628 (1961)].
¹⁶J.R. Schrieffer, *Theory of Superconductivity* (Benjamin, New York, 1964).
¹⁷G.D. Mahan, *Many-Particle Physics*, 2nd ed. (Plenum, New York, 1990), p. 829.
¹⁸D.N. Basov, R. Liang, D.A. Bonn, W.N. Hardy, B. Dabrowski, M. Quijada, D.B. Tanner, J.P. Rice, D.M. Ginsberg, and T. Timusk, Phys. Rev. Lett. **74**, 598 (1995).
¹⁹D.A. Bonn, S. Kamal, K. Zhang, R. Liang, W.N. Hardy, J. Phys. Chem. Solids **56**, 1941 (1995).
²⁰K. Zhang, D.A. Bonn, S. Kamal, R. Liang, D.J. Baar, W.N. Hardy, D. Basov, and T. Timusk, Phys. Rev. Lett. **73**, 2484 (1994).